International Journal of Engineering Trends and Technology
ISSN: 2231 – 5381 / https://doi.org/10.14445/22315381/IJETT-V70I10P211

Volume 70 Issue 10, 87-97, October 2022

Original Article

Experiment on Sensorless Control of an Induction Motor using Backpropagation Neural Network

Pham Thi Giang[1], Vo Quang Vinh[2], Tran Thuy Van[3], Vo Thanh Ha[4*]

[1]*Faculty of Electrical, University of Economics - Technology for Industries, VietNam*
[2]*Faculty of Control and Automation, Electric Power University, Vietnam*
[3]*Faculty of Electrical Engineering, Hanoi University of Industry, Vietnam*
[4*]*Faculty of Electrical and Electronic Engineering, University of Transport and Communications, VietNam*

[4*]*Corresponding Author : vothanhha.ktd@utc.edu.vn*

Received: 05 July 2022 Revised: 25 September 2022 Accepted: 07 October 2022 Published: 19 October 2022

Abstract - *A three-phase induction motor is commonly utilized in industrial and electric vehicles. Furthermore, electric drive systems without speed sensors are becoming more popular because of their small size, cheap cost, outstanding dependability, and sustainability combined with innovative algorithms and controls. As a result, speed estimate techniques are used in these sensorless drive systems instead of direct speed measuring equipment like tachometers or photoelectric encoders. Based on an artificial neural network, this research proposes a technique for estimating the speed of a three-phase asynchronous motor without a speed sensor. The engine's speed determines the neural network's weight, and the real-time error backpropagation algorithm updates the sample period. They are using experiments with the suggested estimate approach. The simulation and experiment findings demonstrate that when the speed response error is estimated using the actual speed using an artificial neural.*

Keywords - *Induction Motor, Neural Network, Luenberger Observer, Kalman Filter Observer, Sliding mode Observer.*

1. Introduction

Induction motors (IM) are becoming more popular in industrial settings. Implementation of oriented field control (FOC) for an induction motor. Induction motors are controlled similarly to individually stimulated DC motors. Consequently, the industry's fundamental and dynamic behavior strength has improved through the orthogonal breakdown of the three-phase current, vector control results in decoupled torque and flux control. The three-phase currents (*ia*, *ib*, *ic*) are split into two orthogonal DC components (*isd*, *isq*), with 'id' controlling the magnetic flux and 'iq' controlling the speed and torque. [1],[2],[3], and [4]. Speed sensors are required for any speed control method for an induction motor drive. On the other hand, sensors add to the system's cost and are unreliable. These drawbacks may be mitigated by using a sensorless technique. The sensorless control operates without the need for a speed sensor. Calculations utilizing observed voltages and currents may predict speed in such instances. On the other hand, sensorless power increases numerical calculations and system complexity [5], [6]. Different approaches available in the literature may be used to provide sensorless control on induction motor drives. The Observer-based method has been the most effective. Observer-based models are state estimators that use input and output data to identify the system's states over a specified period. The observers were created for sensorless induction motor drive control and to assess the speed of IM. The Luenberger observer and Kalman filter versions have been extensively studied for sensorless IM drives. Even though these approaches have been successfully implemented for sensorless operation [5],[6], and [7], they impose a high computing cost, and Kalman filter tuning is a surprisingly sophisticated and time-consuming task. Both observers require an accurate mathematical IM model [8],[9], and [10]. Another study, according to [27], this study analyzes three types of observers placed in a sensorless DFOC IM drive such as Luenberger observer (LO), sliding mode observer (SMO), and Kalman filter (KF). Each observer can give excellent performance at high speeds, and adding the load torque observation improves the dynamic performance of the speed estimate. The LO has the best steady-state performance and low-speed operating [12], [13], and [14]. The SMO has the comparable overall performance to LO. However, it is more parameter-resistant. Digital signal processing for KF is the most difficult to implement. Its low-speed performance is noticeably worse, particularly under load. KF, on the other hand, offers the best noise isolation. In terms of practical use, LO and SMO are more valuable than KF [15],[16],[17],[18] and [19].

Artificial intelligence methods are now used to simulate human behavior and reasoning capacities and implant them into computer programs. In power electronics, AI roaches are becoming more popular. One such AI method is the artificial neural network (ANN), with several benefits [20],[21], and [22]. Self-learning and self-organizing capabilities are two of ANN's most prominent qualities. As a result, it may be used to create an observer based on ANN [23],[24],[25], and [26].

Furthermore, the system benefits from not requiring an accurate mathematical model and is mathematically less demanding. This study created an ANN-based observer for sensorless control of the IM. Furthermore, a flatness technique controller was used to regulate the speed.

There are five parts to this study. First, the induction motor model is provided in section II after the introduction. Next, the backpropagation neural network observer is available in section III. Finally, the simulation results are presented in part IV, followed by conclusions in section V.

2. The Dynamic Mode of an Induction Motor

A general dynamic model of the engine three-phase synchronization includes the following submodules:

- Electrical model for converting three phases to two axes coordinates of the stator voltage.
- The torque model used to calculate electric torque is from.
- Mechanical model for calculating rotor speed.
- Calculation model of stator current when taking into account resistance of a connecting wire

2.1. Electric Model

The process of converting three-phase power supply voltage to voltages in the d and q coordinate systems is taken in the matrix equation below:

$$\begin{bmatrix} V_{ds} \\ V_{qs} \end{bmatrix} = \begin{bmatrix} 1 & -1/2 & -1/2 \\ 0 & \sqrt{3}/2 & -\sqrt{3}/2 \end{bmatrix} \begin{bmatrix} V_{as} \\ V_{bs} \\ V_{cs} \end{bmatrix} \quad (1)$$

Where: V_{as}, V_{bs} and V_{cs} are three-phase stator voltages, while V_{ds} and V_{qs} are biaxial voltage vector components. In a two-axis frame of reference, the equation th current has the following form:

Where R_s and R_r are the stator and rotor resistance, respectively, L_s, L_r and L_m are the stators, rotors, and support inductances, respectively, having a cold. p is the number of poles and ωr is the speed of the rotor. In the electric model, the three-phase voltage [V_{as}, V_{bs}, V_{cs}] is the input, and the current vector [i_{ds}, i_{qs}, i_{dr}, i_{qr}] is the output. Vector the rotor voltage is normally zero due to the rotor having squirrel cage form, that is, $V_{dr} = V_{qr} = 0$.

$$\begin{bmatrix} i_{ds} \\ i_{qs} \\ i_{dr} \\ i_{qr} \end{bmatrix} = \int_0^\tau \left\{ \begin{bmatrix} L_s & 0 & L_m & 0 \\ 0 & L_s & 0 & L_m \\ L_m & 0 & L_r & 0 \\ 0 & L_m & 0 & L_r \end{bmatrix}^{-1} \times \left(\begin{bmatrix} V_{ds} \\ V_{qs} \\ V_{dr} \\ V_{qr} \end{bmatrix} - \begin{bmatrix} R_s & 0 & 0 & 0 \\ 0 & R_s & 0 & 0 \\ 0 & \frac{p}{2}\omega_r L_m & R_r & \frac{p}{2}\omega_r L_r \\ -\frac{p}{2}\omega_r L_m & 0 & -\frac{p}{2}\omega_r L_r & R_r \end{bmatrix} \begin{bmatrix} i_{ds} \\ i_{qs} \\ i_{dr} \\ i_{qr} \end{bmatrix} \right) \right\} d\tau \quad (2)$$

2.2. Torque Model

In the two-axis stator reference frame, the electromagnetic torque M is calculated as follows:

$$M = \frac{pL_m}{3}(i_{dr} i_{qs} - i_{qr} i_{ds}) \quad (3)$$

2.3. Mechanical Model

From the moment equilibrium equation and ignoring friction viscous friction), the rotor speed is calculated as follows:

$$\omega_r = \int_0^\tau \frac{M - M_l}{J} d\tau \quad (3)$$

Where: J is the rotor moment of inertia, and M_L is load torque.

2.4. The Stator Current Model

The stator current model is used to calculate the amplitude stator current according to the following equation:

$$|i_s| = \frac{2}{3}\sqrt{i_{ds}^2 + i_{qs}^2} \quad (4)$$

2.5. Power Supply Model

The power supply to the motor is a sinusoidal three-phase source like after:

$$V_{as} = |V|\, cos(\omega t + \theta)$$
$$V_{bs} = |V|\, cos(\omega t - 2\pi/3 + \theta)$$
$$V_{cs} = |V|\, cos(\omega t + 2\pi/3 + \theta) \quad (5)$$

Where: $|V|$ is the terminal voltage amplitude, ω is the power supply frequency, and θ is the initial phase angle. Due to the voltage drop across the conductor, the terminal voltage is calculated as follows:

$$|V| = E - R_c|i_s| \quad (6)$$

Where: E is the supply voltage, and R_c is the wire resistance connect.

3. Estimated an Induction Motor used Backpropagation- Neural Network

Estimated motor speed using a neural network is part of the adaptive model reference system (model reference adaptive system/MRAS). Here, the neural network serves as

an adaptive model (adaptive model). Neural network consisting of weights constant weights and adjustable weights (adjustable weights).

Correction weights are proportional to rotor speed and sampling time T_s. Figure.1 is the set MRAS-based engine speed estimation, including a neural network trained with the wrong algorithm backpropagation number.

Reference model outputs (Reference Model) are the leakage flux components in the frame of reference static is calculated as follows:

$$\psi_{dr} = \frac{L_r}{L_m}[\int(V_{ds} - R_s i_{ds})dt - L_s^{'} i_{ds}] \quad (7)$$

$$\psi_{qr} = \frac{L_r}{L_m}\left[\int(V_{qs} - R_s i_{qs})dt - L_s^{'} i_{qs}\right] \quad (8)$$

Where: $L_s' = \sigma L_s$with $\sigma = 1 - \frac{L^2 m}{L_r L_s}$is called the word coefficient leak. It is easy to see that Eqs. (8) and (9) do not contain rotor speed. On the other hand, the equations of the model adaptation have the following form:

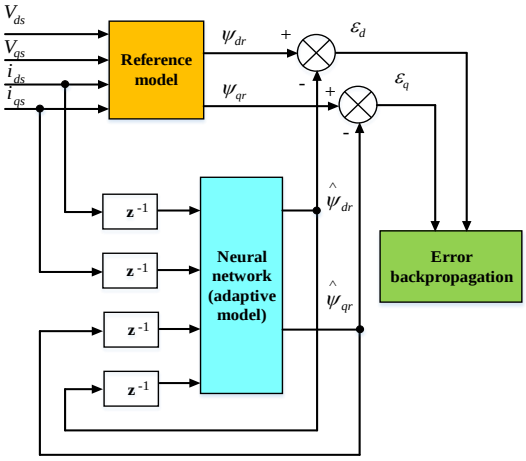

Fig. 1 The speed estimator structure

$$\hat{\psi}_{dr} = \frac{1}{T_r}\int\left(L_m i_{ds} - \hat{\psi}_{dr} - \omega_r T_r \hat{\psi}_{qr}\right)dt \quad (9)$$

$$\hat{\psi}_{qr} = \frac{1}{T_r}\int\left(L_m i_{qs} - \hat{\psi}_{qr} + \omega_r T_r \hat{\psi}_{dr}\right)dt \quad (10)$$

From Eqs. (10) and (11), it can build an artificial neural network consisting of weights as follows:

$w_1 = 1 - c$, $w_2 = \omega_T.T_s$, $w_3 = cL_m$. In there $c = T_s/T_r$with T_s is the time is taken form and $T_r = L_r/R_r$ the rotor's electromagnetic time constant. The weight w_2 is proportional to the rotor speed and sampling cycle. For a particular application, the cycle sampling is unchanged. Therefore, the weight value w_2 will be adjusted for the rotor speed. By method back difference method, the system the output equation of the adaptive model is from leakages at k sampling time is as follows:

$$\hat{\psi}_{dr}(k) = w_1\hat{\psi}_{dr}(k-1) - w_2\hat{\psi}_{qr}(k-1) + w_3 i_{ds}(k-1) \quad (11)$$

$$\hat{\psi}_{qr}(k) = w_1\hat{\psi}_{qr}(k-1) + w_2\hat{\psi}_{dr}(k-1) + w_3 i_{qs}(k-1) \quad (12)$$

Eqs. (12) and (13) can be represented in the form of an artificial neural network with a graph like Fig.2. Finally, the rotor speed is estimated at the k sampling time is determined as follows:

$$\hat{\omega}_r(k) = \hat{\omega}_r(k-1) + \frac{\eta}{T_s}\begin{pmatrix}\left[\psi_{qr}(k) - \hat{\psi}_{qr}(k)\right]\hat{\psi}_{dr}(k-1) \\ -\left[\psi_{dr}(k) - \hat{\psi}_{dr}(k)\right]\hat{\psi}_{qr}(k-1)\end{pmatrix} \quad (13)$$

Here η is the learning rate.

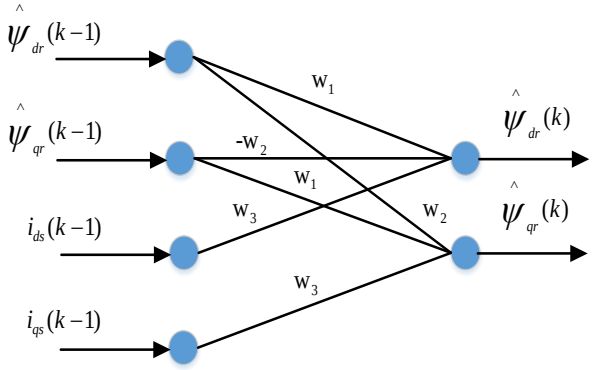

Fig. 2 Neural network graph used to estimate the flux

4. Results

The simulations are carried out on an induction machine using the settings listed in Table 1. Fig. 9 depicts the construction of the test bench.

4.1. Simulation Results

4.1.1. Case 1: Consider the hypothetical case that the engine parameters' IM does not change

The article selects a stator PI current controller with the coefficient K_p=20; T_i=0.0085; PI speed controller with factor K_p=200; T_i=0.002 [6]. The operating mode of the IM motor is in the basic speed range and is investigated through the simulation scenarios as follows:

Table 1. Design specification of an induction motor

Rated power	P_{dm}	2.2kW
Rated Torque	M_{dm}	7.3Nm
Rated phase current	I_{dm}	4.7A
Rated phase voltage	U_{dm}	400V
Rated frequency	f_{dm}	50Hz
Number of pole pairs	p	1
Stator resistance	R_s	1.99Ω
Rotor resistance	R_r	1.84Ω
Mutual inductance	L_m	0.37
Rated speed	n_{dm}	2880 rpm
Torque of inertia	J	$Kg.m^2$

At time t = 0s, magnetization occurs, and the rotor flux stabilizes after a while, followed by at t = 1s starting and increasing motor speed (150 rad/s) and at t= 3s proceeding to reverse the motor (-150 rad/s).

The stator current /variable accuracy simulation results and decoupling at point operations, such as stability, speed up, and speed down, are shown in Figures 3 and 4. It does, however, include overshoots during the transition response.

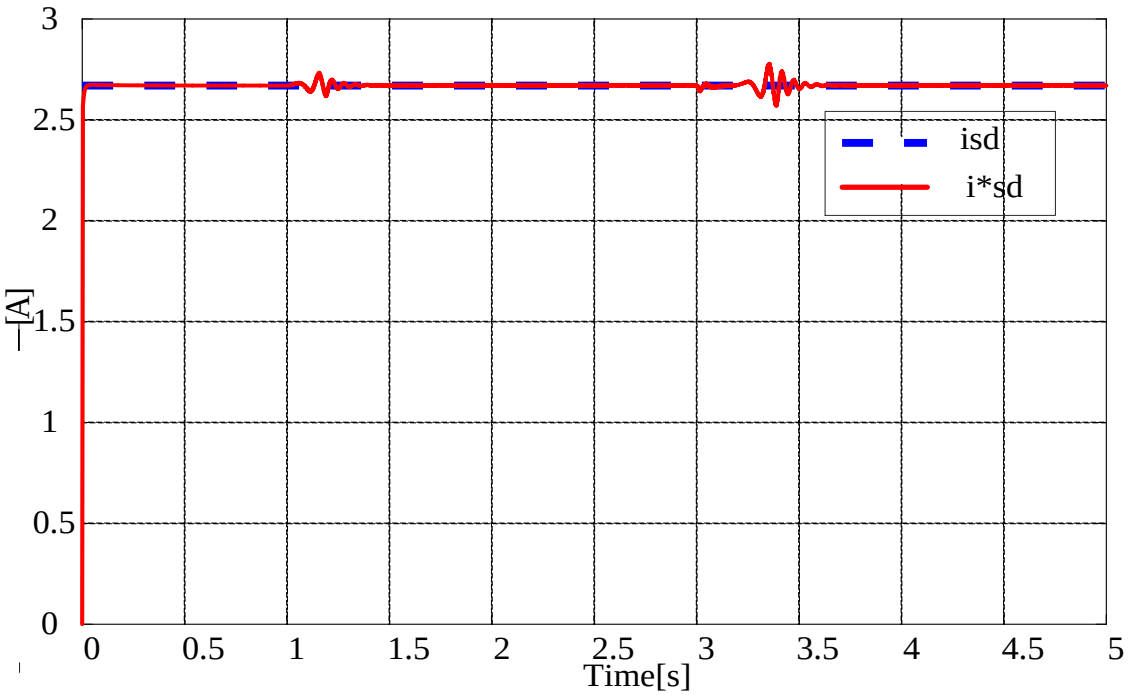

Fig. 3 The current response $i_{sd}^{*} - i_{sd}$

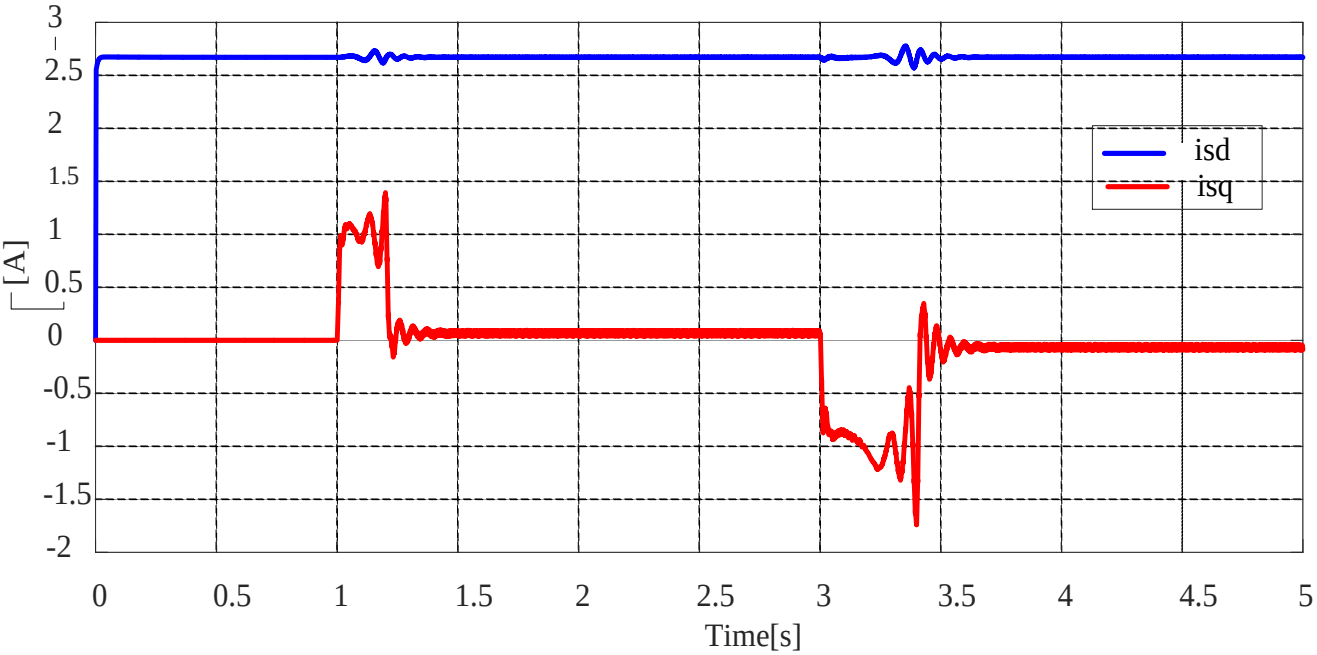

Fig. 4 The current response i_{sd} - i_{sq}

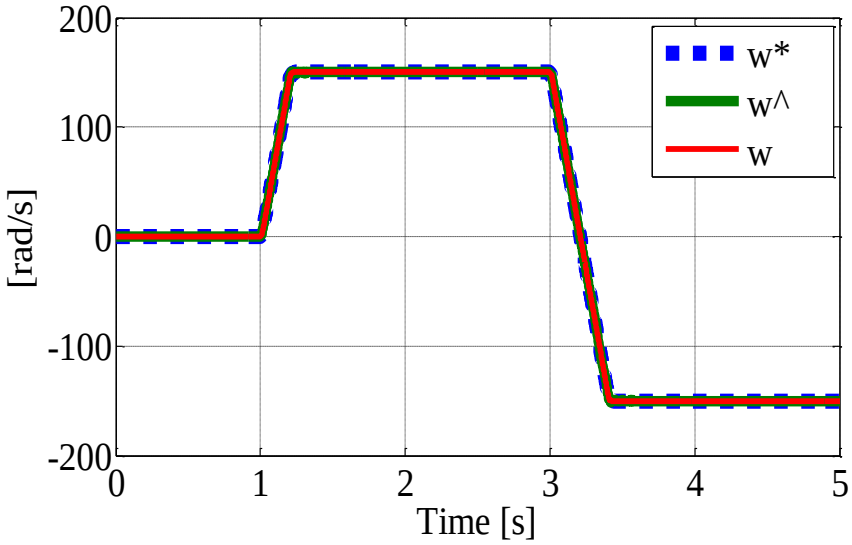

Fig. 5 The speed response (reference w*; estimate w^; motor w)

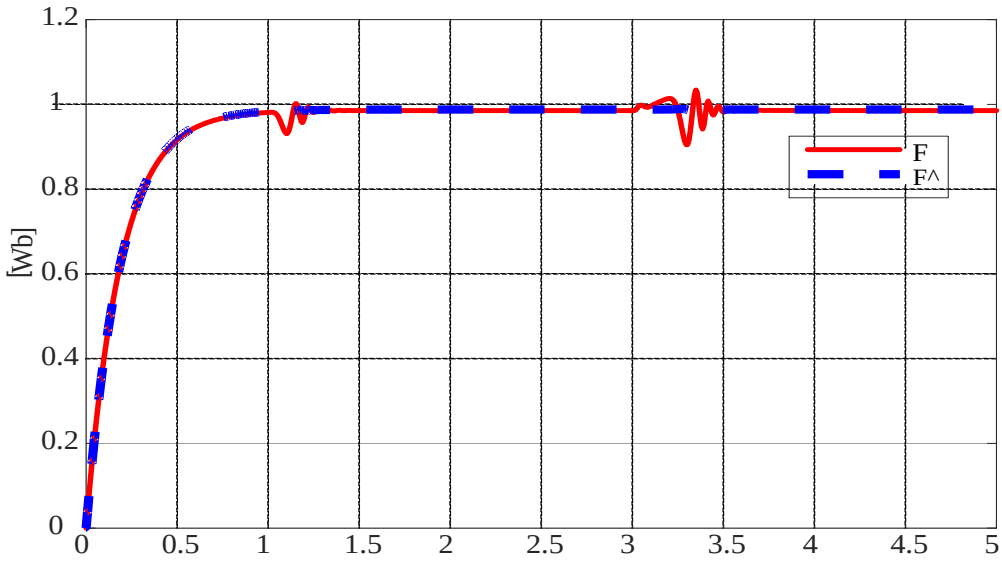

Fig. 6 The flux response (calculator F; estimate F^)

Figs.5 and 6 show the simulation results procedures, respectively. The gap between the actual speed and flux and the anticipated speed and flux shows that the online neural network speed and flux estimator can accurately estimate the speed and flux in speed ranges. In transient processes, estimate errors are relatively tiny and near zero in steady-state activities.

Fig. 5 and 6 show the simulation results procedures, respectively. The gap between the actual speed and flux and the anticipated speed and flux shows that the online neural speed and flux estimator can accurately estimate the speed and flux in high-speed ranges. In transient processes, estimate errors are relatively tiny and near zero in steady-state activities. However, at transients (acceleration and deceleration) during the operation of the IM motor, the speed and flux responses appear slightly overshoot.

4.1.2. Case 2: Consider the hypothetical case that the engine parameters' IM does change

When the IM motor works for a long time, the rotor resistance increases, resulting in a change in the rotor time constant and flux and decreased motor speed. For example, research work with the case of rotor resistance increased by 50%. The results of the stator's current response rate are shown in the following figures:

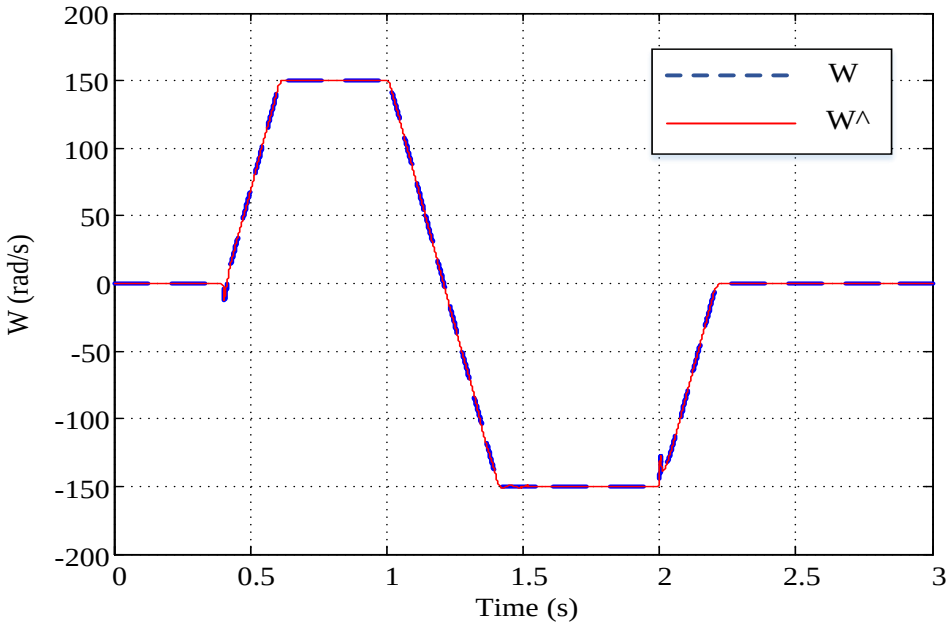

Fig. 7 The speed response (estimate w^; motor w) when Rr is increased by 50%

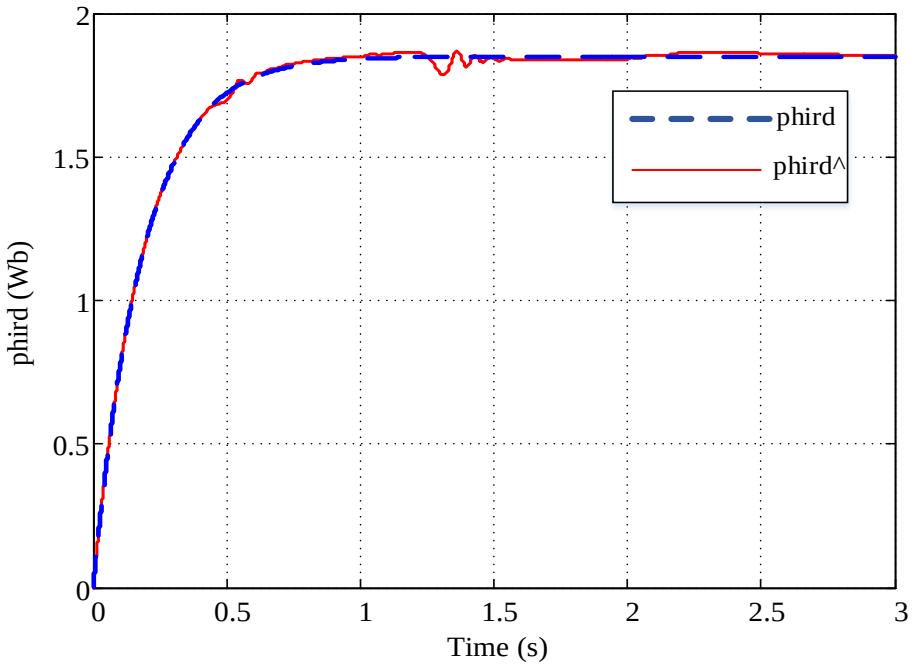

Fig. 8 The flux response (estimate w^; motor w) when Rr is increased by 50%

The results of Fig. 7 show that the estimated speed is close to the actual engine speed. For example, setting the resisting torque t = 0.4s and the time of deceleration t = 2s, the adjustment output is 20%. Besides, the simulation results of Fig. 8 show that the estimated and calculated flux are closely followed. The error only occurs in the 20% transition. Proving that the neural network observer works effectively.

4.2. Experimental Results

On the DSP 1104, all control, stator flux estimation, and speed estimate algorithms are conducted. The sample time is 200 µs to guarantee adequate time for algorithm processing, data collecting, and converting analog to digital converters (ADC) and digital to analog converters (DAC). Furthermore, for high, the speed standards are stepped from a standstill to 150 rad/s, and for low, from a standstill to – 150 rad/s.

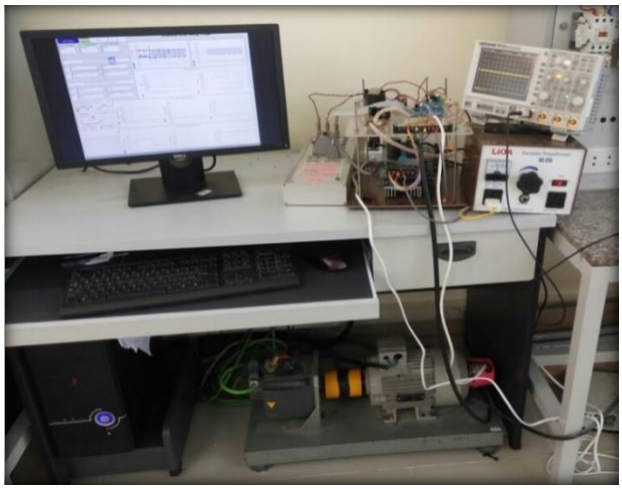

Fig. 9 Photo of the experimental setup

The experiments are carried out on an induction machine using the settings listed in Table 1.

4.2.1. Case 1: *Consider the hypothetical case that the engine parameters' IM does not change.*

Experimental results of stator current response are shown in Figs.10, 11. Through experimental results, it is found that the stator current response controls the flux, and the torque does not change during the setting process, with the difference between the actual and set stator current response being zero, but at the time of over speed (acceleration and reverse) occurs 20% over-adjustment. Still, after 0.5s, the actual stator current closely follows the set value. This result shows that the magnetic flux has been correctly estimated, and the PI current controller has realized the instability and torque control demultiplexing. However, the interleaving phenomenon still exists when the motor is running. Act at the moment of transition. Therefore, it is necessary to have a solution to design the current controller so that the responses are fast and accurate.

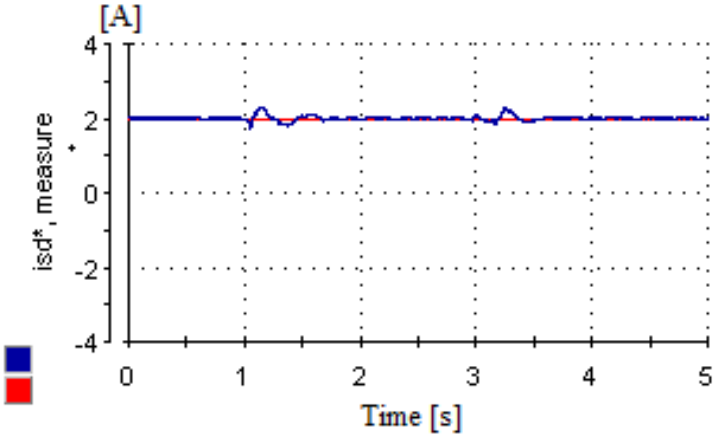

Fig. 10 The current response $i_{sd}^{*} - i_{sd}$

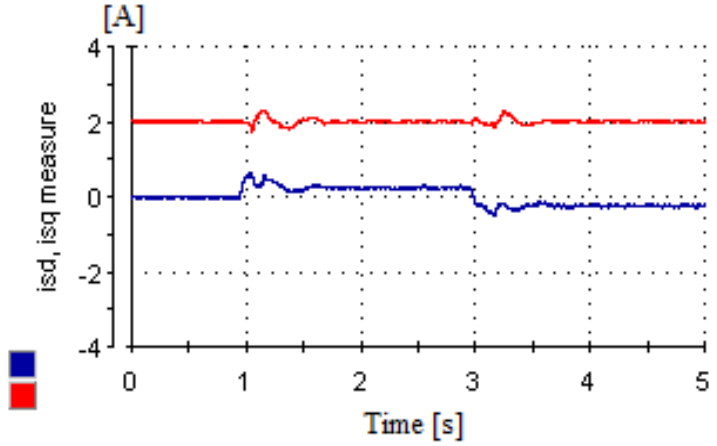

Fig. 11 The current response $i_{sd} - i_{sq}$

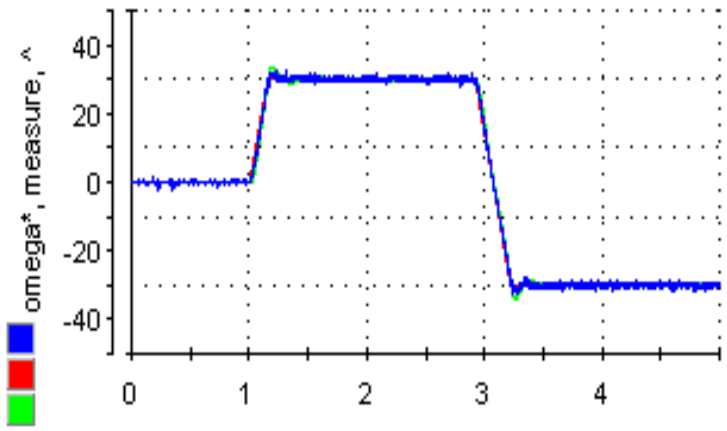

Fig. 12. The speed response w, w* and w^.

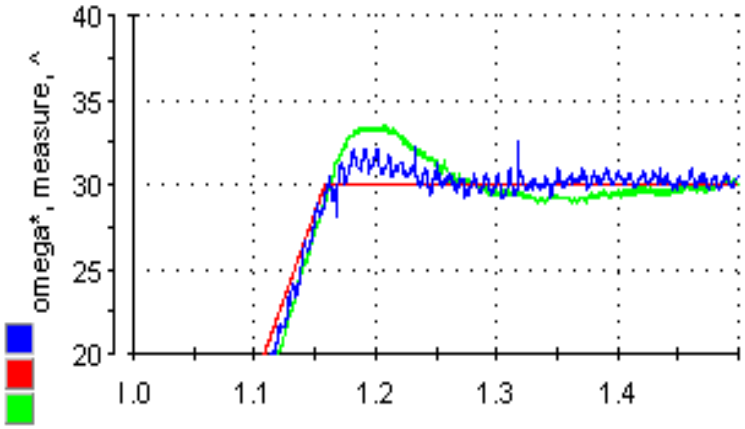

Fig. 13 The enlarged image responds to setting, measuring, and estimating speed when the motor starts up

In addition, the set, measured, and estimated speed responses are shown in Fig.12, and an enlarged image of the speed responses (reference, measure, and estimate) is in Fig. 13. Through the results of Figs. 12 and 13, there are found that the estimated speed is close to the set value, measured at steady-state, but at the time of start-up and reverse, the estimated speed response appears to overshoot by about 6%, but quickly after 0.2s then meet the estimated speed as required. Therefore, prove that the speed monitor is well-designed and responsive to the requirements.

4.2.2. Case 2: Consider the hypothetical case that the engine parameters' IM does change.

In the field, when rotor resistance increases, the experimental results of stator current response control flux and torque are shown in Figs. 14.15. This result indicates that the stator current response has a higher pulse rate than the above field. In addition, the stator current response is highly overcorrected (40%). Finally, there is an inter-channel phenomenon between the stator currents i_{sd} and i_{sq}, but the real signal generator adheres to the set value with almost zero error. These results show that the rotor flux estimator design responds well to the drive system with variable motor parameters.

Similar to case 1, the reference, measured, and estimated rate responses are shown in Figs. 16 and 17. These rate responses have the same shape at steady-state but at the time of transition. Then the overcorrection is as large as 50%. After 0.5s, the establishment process occurs. The speed monitor still works well even when the engine parameter (Rr) changes.

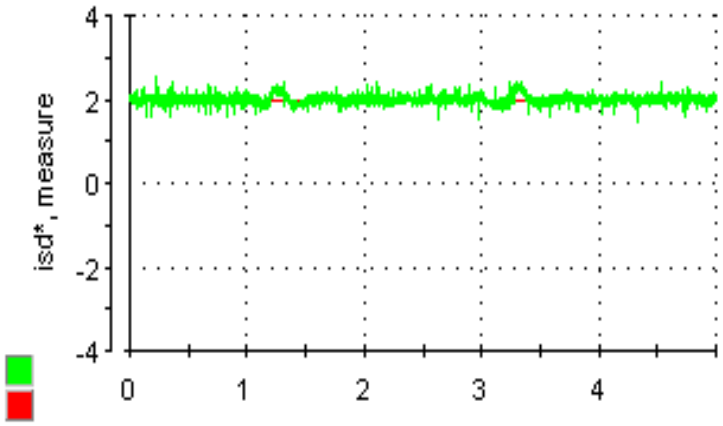

Fig. 14 The Stator current response when Rr is increased by 50%

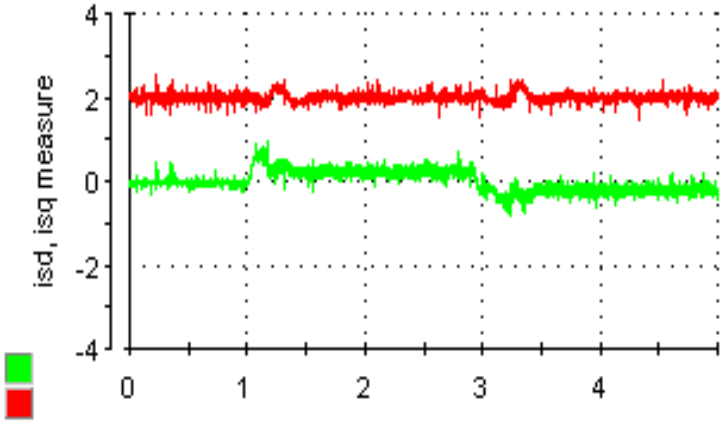

Fig. 15 The enlarged image responds to a 50% increase in Rr set, measures and estimates speed

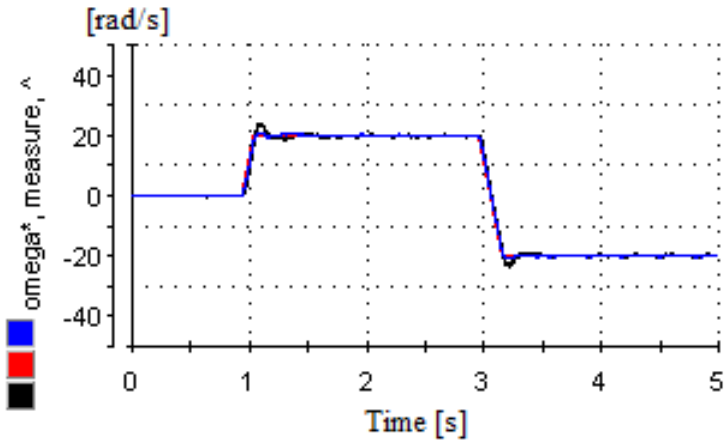

Fig. 16 Reference, measure, and estimate rate response when R_r

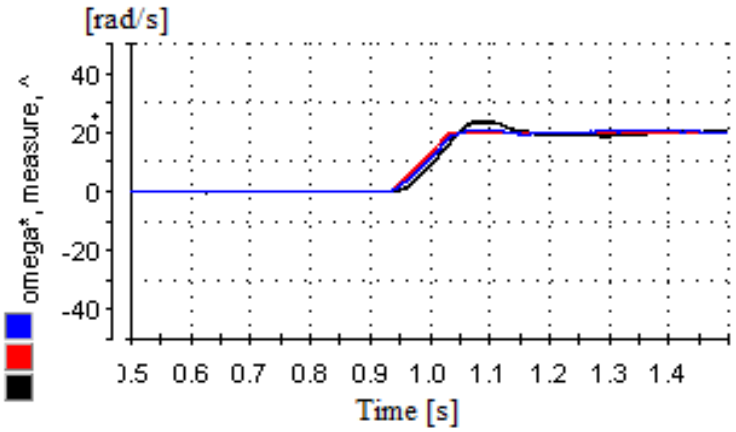

Fig. 17 Enlarged image responds to set, measure and estimate speed as Rr increases by 50%- IM engine start

5. Conclusion

This study proposes an online neural network speed estimator for three-phase IM speed sensorless direct torque control using the FOC control approach. The modeling and experimental findings demonstrate that the speed and flux estimators can adequately predict the rate and flux in speed locations. Furthermore, the control system incorporated into the supplied speed estimator is stable and has rapid dynamic reactions and exact steady-state responses. These findings support the use of the recently proposed online neural network speed estimator. However, the estimate errors from experimental findings in speed areas are different from the simulation results in transitory settings, such as when the motor begins and reverses.

References

[1] Nguyen Phung Quang, Jorg-Andreas Dittrich, "Vector Control of Three-Phase AC Machines, System Development in the Practice," *Springer*, 2015.

[2] Leonhard W, "Control of Electrical Drives," 2nd Edition, *Springer*, 1996.

[3] T.Ohtani, N.Takada, "Vector Control of Induction Motor Without Shaft Encoder," *In Conf. Rec. 1989 IEEE IAS Annual Mtg*, pp.500-507.

[4] A. Hinda, M. Khiat, And Z. Boudjema, "Advanced Control Scheme of a Unified power Flow Controller using Sliding Mode Control," *International Journal of Power Electronics and Drive Systems (IJPEDS)*, vol. 11, no. 2, pp. 625-633, 2020. Doi: 10.11591/IJPEDS.V11.I2.PP625-633.

[5] J. Holtz, "Sensorless Control Of Induction Machines—With or Without Signal Injection," *IEEE Transactions on Industrial Electronics*, vol. 53, no. 1, pp. 7–30, 2006.

[6] Vo Thanh Ha; Nguyen Van Thang; Duong Anh Tuan; Pham Thi Hong Hanh, " Sensorless Speed Control of aThree-Phase Induction Motor: An Experiment Approach," *2017 International Conference on System Science and Engineering* (*ICSSE*).

[7] Zineb Kandoussi; Zakaria Boulghasoul; Abdelhadi Elbacha; Abdelouahed Tajer, "Luenberger Observer Based Sensorless Indirect Foc With Stator Resistance Adaptation," *2014 Second World Conference on Complex Systems* (*WCCS*).

[8] Juraj Gacho, Milan Zalman, " Im Based Speed Servodrive With Luenberger Observer," *Journal of Electrical Engineering*, vol. 61, no. 3, 2010.

[9] Vo Thanh Ha, Nguyen Tung Lam, Pham Van Tuan, Nguyen Hong Quang, "Experiments Based Comparative Analysis of Nonlinear Speed Control Methods For Induction Motors," *Journal of Engineering and Technological Sciences*, vol. 53, no. 2, 2021.

[10] Vo Thanh Ha; Nguyen Tung Lam; Vo Thu Ha; Vo Quang Vinh, "Advanced Control Structures For Induction Motors With Ideal Current Loop Response Using Field Oriented Control," *International Journal of Power Electronics and Drive System* (*IJPEDS*) vol. 10, no. 4, pp. 1758-1771, 2019. Issn: 2088-8694, Doi: 10.11591/IJPEDS.V10.I4.PP1758-1771.

[11] Vo Quang Vinh, Pham Thi Hong Hanh, Vu Thi Kim Nhi, "Speed Estimation For Induction Motor Using Model Reference Adaptive System and Fuzzy Logic Controller," *SSRG International Journal of Electrical and Electronics Engineering*, vol. 6, no. 3, pp. 1-9, 2019. Crossref, https://doi.org/10.14445/23488379/IJEEE-V6I3P102.

[12] Yongchang Zhang, Zhengming Zhao, Ting Lu, Liqiang Yuan, "A Comparative Study of Luenberger Observer, Sliding Mode Observer and Extended," *IEEE*, 978-1-4244-2893-9/09/$25.00 , 2009.

[13] Ali Saffet Altay, Mehmet Emin Tacer, Ahmet Faik Mergen, "Sensorless Speed Control of A Vector Controlled Three-Phase Induction Motor Drive By Using MRAS," *Journal of Vibro Engineering*, vol. 16, no. 3, 2014, pp. 1258-1267.

[14] Mabroukjouili, Kameljarray, Yassinekoubaa, Mohamed Boussak, "Luenberger State Observer for Speed Sensorless ISFOC Induction Motor Drives," *Electric Power Systems Research*, vol. 89, pp. 139-147, 2012.

[15] Murat Barut, Seta Bogosyan, M. Gokasan, "Speed-Sensorless Estimation for Induction Motors using Extended Kalman Filters," *IEEE Transactions on Industrial Electronics*, vol.54, no. 1, pp. 272 – 280, 2007.

[16] Vishal Tiwari, Sukanta Das, Abhisek Pal, "Sensorless Speed Control of Induction Motor Drive using Extended Kalman Filter Observer," Conference: *Ieee PES Asia-Pacific Power and Energy Engineering Conference* (*APPEEC*), 2017.

[17] Jongkwan Kim, Yongkeun Lee, Janghyeon Lee, "A Sensorless Speed Estimation for Indirect Vector Control of Three-Phase Induction Motor Using Extended Kalman Filter," *Published 1 November 2016 Engineering 2016 IEEE Region 10 Conference* (TENCON).

[18] Mohammad Jannati, Ali Monadi, Nik Rumzi Nik Idris, Mohd Junaidi Abdul Aziz, "Speed Sensorless Vector Control of Unbalanced Three-Phase Induction Motor With Adaptive Sliding Mode Control," *International Journal of Power Electronics and Drive System (IJPEDS)* vol. 4, no. 3, pp. 406-418, 2014. ISSN: 2088-8694.

[19] Akashp P, Mahadevi Biradarp, "Speed Sensorless Vector Control of Induction Motor using Reduced Order Extended Kalman Filter," *IJISET - International Journal of Innovative Science, Engineering & Technology*, vol. 3, no. 11, 2016. ISSN (Online) 2348 – 7968 | Impact Factor (2015) - 4.332.

[20] S. M. Gadoue, D. Giaouris and J. W. Finch, "Sensorless Control of Induction Motor Drives At Very Low and Zero Speeds Using Neural Network Flux Observers," IEEE Transactions on Industrial Electronics, vol. 56, no. 8, pp. 3029-3039, 2009.

[21] G. Liu, Z. Hu, Y. Shen, H. Zhou, and C. Teng, "Estimation of Induction Motor Speed Based on Artificial Neural Networks Inversion System," *International Conference on Neural Networks and Signal Processing*, pp. 43 - 47, 2008.

[22] S. M. Gadoue, D. Giaouris and J. W. Finch, "Sensorless Control of Induction Motor Drives At Very Low and Zero Speeds Using Neural Network Flux Observers," *IEEE Transactions on Industrial Electronics*, 2009.

[23] Seong-Hwan Kim, Tae-Sik Park, Ji-Yoon Yoo, and Gwi-Tae Park, "Speed-Sensorless Vector Control of An Induction Motor Using Neural Network Speed Estimation," *IEEE Transactions on Industrial Electronics*, vol. 48, no. 3, pp. 609, 2001.

[24] Siddanna Dhavalagi, Dr. Basavaraj Amarapu, "CMAC Neural Network Based Speed Control of Induction Motor," *IJSRD - International Journal For Scientific Research & Development*, vol. 5, no. 09, 2017. ISSN (Online): 2321-0613.

[25] M. Elgohary, E. Gouda, S. S. Eskande, "Intelligent Control of Induction Motor Without Speed Sensor," *International Journal of Power Electronics and Drive Systems* (*IJPEDS*) vol. 12, no. 2, pp. 715-725, 2021. Issn: 2088-8694, Doi: 10.11591/IJPEDS.V12.I2.PP715-725.

[26] Pranav Pradip Sonawane, 2mrs. S. D. Joshi, "Sensorless Speed Control of Induction Motor by Artificial Neural Network," *International Journal of Industrial Electronics and Electrical Engineering*, vol. 5, no. 2, 2017.

[27] José L. Mora, A. Torralba, L. G. Franquelo, "A Speed Adaptive Kalman Filter Observer for Induction Motors," All Content Following This Page Was Uploaded By Leopoldo Garcia Franquelo on 03 November 2014.